Dynamical Behaviour of Pro- and Anti-Inflammatory Cytokines during Pathogenesis of Atherosclerosis

Asish Adak[1], **Arpita Devi**[1], **Praveen Kumar Gupta**[1*]

[1]Department of Mathematics, National Institute of Technology Silchar, Assam 788010, India

[*]Email: praveen@math.nits.ac.in

Abstract

The role of anti-cytokines in atherosclerosis is to reduce inflammation in the intima. In some situations, certain anti-inflammatory cytokines like TGF-beta and IL-6 have shown the characteristics like a pro-inflammatory cytokines, which are showing different natures. In this study, a dynamical atherosclerosis model is proposed in the form of reaction-diffusion equation with consideration of immune cells, pro-inflammatory cytokines, and anti-inflammatory cytokines. The existence and uniqueness of the solutions are discussed for the proposed reaction dynamical system. The three equilibrium points, non-inflammatory, chronic, and coexistence, and their local stability are also determined for the model. Bellman and Cooke's theorem is applied to illustrate the global stability at the coexistence equilibrium point. The effects of pro- and anti-inflammatory cytokines have also been discussed. The analytical and numerical studies evidently indicate that inflammation behaves differently when a certain number of anti-inflammatory cytokines behave like pro-inflammatory cytokines. The numerical simulations are demonstrated for different impacts of the reduction rate of macrophages due to the presence of anti-inflammatory cytokines, inhibition time, and the portion of anti-inflammatory cytokines behaving like pro-inflammatory cytokines through graphically. The results of this study suggest that chronic inflammation of the disease is likely to persist when a high concentration of ox-LDL and moderate concentration of cytokines are present in the intima. Coexistence inflammation is characterized by a high concentration of ox-LDL, moderate concentration of pro-inflammatory and high concentration of anti-cytokines; whereas a non-inflammatory condition would persevere if a low concentration of ox-LDL has been present in the intima.

Keywords: Bellman-Cooke's theorem, cytokines, reaction-diffusion equation, immune cells, pro and anti-inflammatory, ox-LDL

2010 MSC classification number: 92B05, 93C20, 93D05

1. INTRODUCTION

The most recent factsheets of the World Health Organization state that about 17.9 million people died of cardiovascular diseases in 2019, which accounts for 32% of all global deaths [1]. Among these, atherosclerotic heart disease (ASCVD) remains a leading cause of death worldwide despite significant advances in diagnosis and treatment procedures. It is a chronic inflammatory disease of the large and medium-sized arteries, which is often responsible for death. In various animal and patient models, it is observed that cardiopalmus or heart beat is also directly associated with coronary atherosclerosis. It has also been confirmed in several studies that if the heart beat is increased then in most cases it is due to the increased progression of coronary atherosclerosis, while lower heart beat is connected with decreased cardiovascular and complications [2], [3]. In these patients, the chances of plaque rupture are very high. Additionally, inflammation contributes significantly to the pathogenesis and progression of atherosclerosis, which makes the disease more severe. In the literature, many researchers considered various risk factors of atherosclerosis disease, such as a rich fatty diet, type-2 diabetes, and many more.

In various treatments, the reduction of atherosclerosis by combining anti-inflammation and inhibition-degradation of the plaque is discussed [4]. In the last decade, Sacks *et* al. [5] have studied saturated fatty acids (SFAs) in rich diets given to humans and found this to be an important factor directly linked to an increase in atherosclerosis. After three years in an experiment on mice, Lian *et* al. [6] replaced this SFA with other SFA, namely polyunsaturated fatty acids, and observed that it could reduce atherosclerosis. As we

[*]Corresponding author

Received March 17^{th}, 2023, Revised June 8^{th}, 2023 (first), Revised July 6^{th}, 2023 (second), Accepted for publication August 21^{st}, 2023. e-ISSN: 2549-2896, DOI:10.5614/cbms.2023.6.2.3

know, statins are a class of drugs used to control atherosclerosis. Basically, it targets HMG-CoA reductase, which acts as an enzyme in the rate-limiting step of cholesterol biosynthesis [7]. Moghaddam *et* al. found that patients with type-2 diabetes are more likely to develop atherosclerosis which can subsequently lead to dementia through various pathways [8].

Various clinical studies have shown that oxidative transformation of LDL plays an important role in the genesis of atherosclerosis. It begins when LDL is modified through endothelial cells during the oxidation process and is rapidly deposited by macrophages, which are the major contributors to foam cell formation [9], [10], [11], [12]. In 1984, Heineke *et* al. [13] found that any alteration of LDL during incubation with arterial smooth muscle cells was affected and supported by increasing Fe and Cu concentration, whereas no effect of Zn was found. In the previous study, Henriksen *et* al. [12] have shown that LDL customized by incubation through endothelial cells or guinea pig arterial smooth muscle cells is more speedily destroyed by macrophages compared to native LDL. LDL modified by incubation with human smooth muscle cells that are incorporated by human monocyte-derived macrophages and resident mouse peritoneal macrophages into larger amounts of cholesterol esters than control LDL.

Cytokines are low-molecular-weight protein intermediaries that more often than not act at small choice between neighboring cells in lymphoid organs or reddened tissues. Cytokines are produced by all kinds of cells implicated in atherosclerosis, which act on different targets applying multiple effects and are mostly responsible for the interaction between endothelial, leucocytes, smooth muscle cells, and other vascular living cells. These cytokines are classified as pro- and anti-atherogenic cytokines, which are two separate groups depending on whether they stimulate or inhibit atherogenesis. The main pro-atherogenic cytokines viz. tumor necrosis factor$-\alpha$, interleukin$-1a$, and 17 are secreted by macrophages, lymphocytes, natural killer cells, and vascular smooth muscle cells, while anti-atherogenic cytokines identified as transforming growth factor$-\beta$ (TGF$-\beta$), interleukin-10 and 35 [14], [15]. Recently, Hafien and Dascalopoulou [16] have discussed studies on canakinumab anti-inflammatory thrombosis outcomes as well as therapeutic agents to specify the inflammatory pathway in atherosclerotic heart disease and demonstrated the effects of various anti-inflammatory agents in patients with ASCVD. In several experimental results, researchers found that pro- and anti-cytokine profile extensively differs between patients with high and low coronary plaque volume. Certain cytokines such as $IL-1a$ and $IL-17$ play a major pro-atherogenic role in vulnerable plaque formation, while MCP-1 cytokine shows paradoxically protective effects [17], [18]. However, in experiments, some researchers observed that different cytokines behave in both natures and whose effects cannot be left forever.

The aim of this study is to express the measures and effects of pro- and anti-inflammatory cytokines with the help of a system of reaction diffusion equation model and to demonstrate an auxiliary approach to their future prediction. The present study is arranged in the following order. The mathematical description of the chronic inflammatory response with the inclusion of biochemical and mechanical parameters is presented in Section 2. In the next Section 3, we express the proposed model in the form of reaction dynamical system and discuss the existence of the solutions, and determine the equilibrium points for the model. Local and global stability analysis of this model is shown in Section 4. Subsequently, we further discuss the numerical results and discussion for the model in Section 5. Finally, we conclude all the results and outcomes in Section 6.

2. MODEL DESCRIPTION

The present study investigates the chronic inflammatory response of atherosclerosis as well as its biochemical and mechanical behaviour. We presented a mathematical model based on several assumptions and taking into account three main compartments namely, immune cells (M), pro-cytokines (P), and anti-cytokines (A), which is shown in Figure 1. This is formulated by a reaction-diffusion system in one-dimensional space with the concentration of immune cells (macrophage, monocytes) and two types of responsible inflammatory cytokines, viz. pro-inflammatory cytokines($IL-1$, TNF$-\alpha$, $IL-12$) [19], [20], and anti-inflammatory cytokines($IL-10$, $IL-6$, TGF$-\beta$) [4], [16], [21]. These two cytokines are secreted by immune cells. In accordance with the inflammatory nature of pro-inflammatory cytokines, these cytokines are specifically responsible for making atherosclerosis worse, while anti-inflammatory cytokines are known to reduce inflammation [14]. To formulate the mathematical problem, we assume that all compartments are diffusing with appropriate diffusion coefficients, here, x is considered between 0 and finite length L.

Table 1: Description of variables and parameters of the model.

Variables / Parameters	Description
M	Concentration of immune cells (macrophage, monocytes)
P	Concentration of pro-inflammatory cytokines
A	Concentration of anti-inflammatory cytokines
α_1	Initial recruitment of immune cells due to presence of ox-LDLs
α_2	Secretion rate of pro-inflammatory cytokines by itself
α_3	Secretion rate of anti-inflammatory cytokines by inflammatory macrophages.
β_1	Activation rate of macrophages promoted by pro-inflammatory cytokines
β_2	Reduction rate of macrophages due to the presence of anti-inflammatory cytokines
λ_1	death rate of immune cells
λ_2	decay rate of pro-inflammatory cytokines
λ_3	decay rate of anti-inflammatory cytokines
τ_1	Mechanical saturation time
τ_2	Time taken to inhibit pro-inflammatory cytokines by anti-inflammatory cytokines
δ	Portion of secreted anti-inflammatory cytokines behaving like pro-inflammatory cytokines
d_1	diffusion coefficient of immune cells
d_2	diffusion coefficient of pro-inflammatory cytokines
d_3	diffusion coefficient of anti-inflammatory cytokines

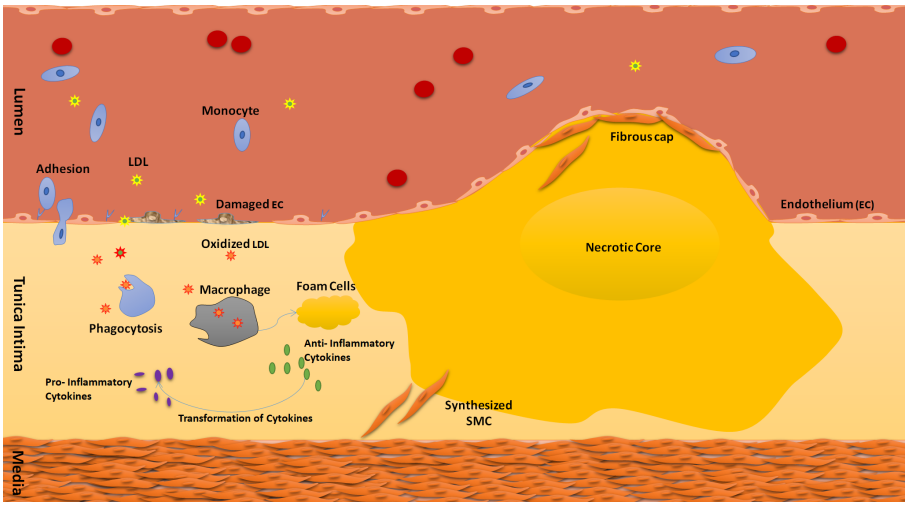

Figure 1: Schematic diagram of Atherosclerosis formation.

2.1. Equation for Immune Cells (M)

The evolution of the immune cells into the intima is defined as

$$\frac{\partial M}{\partial t} = d_1 \frac{\partial^2 M}{\partial x^2} + \frac{\alpha_1 + \beta_1 P - \beta_2 A}{1 + \dfrac{(P+A)}{\tau_1}} - \lambda_1 M. \tag{1}$$

Here, the first term on the right-hand side describes the diffusion of immune cells. The second term is considered as a Beddington-DeAngelis type of functional response [22], [23] which is used for competitive exclusion and coexistence in this model that also involves mutual interference of both immune cells and

cytokines. The third term stands for the degradation of Immune cells. The functional response in the second term is considered through the following factors:

1) α_1 corresponds to the initial recruitment of immune cells due to the existence of unnecessary ox-LDLs [14], [24].
2) $\beta_1 P$ represents the evolution of immune cells promoted by pro-inflammatory cytokines [14], [25].
3) The term $\beta_2 A$ opposes the secretion of immune cells due to the presence of anti-inflammatory cytokines [24], [26].
4) $1 + (P + A)/\tau_1$ is the mechanical saturation factor of the immune cells, where τ_1 is the time taken for the saturation [25].

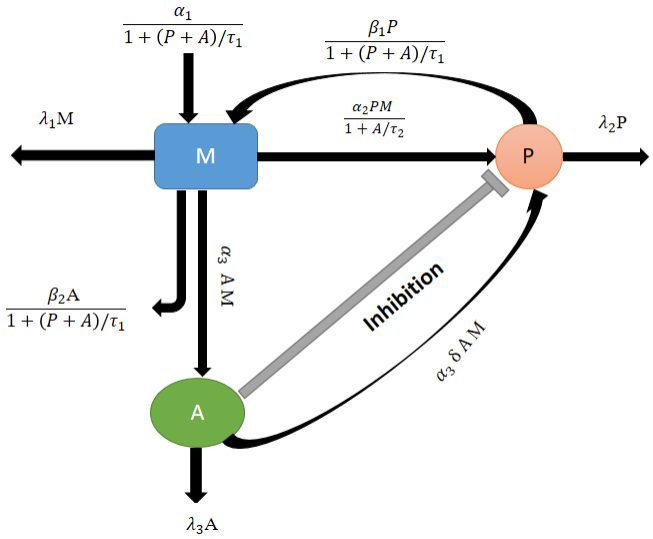

Figure 2: Compartmental flow-chart diagram of the model.

2.2. Equation for Pro-inflammatory Cytokines (P)

The formation of pro-inflammatory cytokines is represented by the following reaction-diffusion equation,

$$\frac{\partial P}{\partial t} = d_2 \frac{\partial^2 P}{\partial x^2} + \frac{\alpha_2 PM}{1 + \dfrac{A}{\tau_2}} + \delta \alpha_3 AM - \lambda_2 P. \tag{2}$$

Here, α_2 is the secretion rate of pro-inflammatory cytokines by itself, $1 + A/\tau_2$ represents the inhibition effect of pro-inflammatory cytokines due to the presence of anti-inflammatory cytokines, τ_2 is the inhibition time to act [14], α_3 is the secretion rate of anti-inflammatory cytokines from immune cells, δ is the ratio of secreted anti-inflammatory cytokines behaving like pro-inflammatory cytokines (TGF-beta, IL-6) [27], [28]. In several studies, IL-6 shows both anti and pro–inflammatory effects during inflammation of atherosclerosis [27], [28].

2.3. Equation for Anti-inflammatory Cytokines (A)

The formation of anti-inflammatory cytokines satisfies the following equation

$$\frac{\partial A}{\partial t} = d_3 \frac{\partial^2 A}{\partial x^2} + (1 - \delta)\, \alpha_3 AM - \lambda_3 A. \tag{3}$$

In general, macrophages are mainly responsible for secretion of cytokines. Here, we consider α_3 is the formation rate of anti-inflammatory cytokines from immune cells.

In the equations (1)-(3), terms $d_1\frac{\partial^2 M}{\partial x^2}$, $d_2\frac{\partial^2 P}{\partial x^2}$ and $d_3\frac{\partial^2 A}{\partial x^2}$ represent the diffusion inside intima, and the terms $-\lambda_1$M,$-\lambda_2$ P and $-\lambda_3$ A represent the decaying rate of the M, P and A, respectively.

In this study, we considered the initial conditions to be a function of x [29],

$$M(0,x) = M_0(x), P(0,x) = P_0(x), A(0,x) = A_0(x), \tag{4}$$

and the homogeneous Neumann boundary conditions,

$$M_x(t,0) = 0, P_x(t,0) = 0, A_x(t,0) = 0, \tag{5}$$
$$M_x(t,L) = 0, P_x(t,L) = 0, A_x(t,L) = 0. \tag{6}$$

The authors are confident that the proposed model (1)–(6) is able to provide new insights into the role of pro- and anti-cytokines in the inflammation and reduction of atherosclerosis.

3. Analysis of the Model

The analytical study of any mathematical model must be a strong and fundamental part of any biological phenomenon that must be clearly described. In this section, we describe the solution of the deterministic atherosclerosis model that always exists or exists with a particular condition. The uniqueness of the solution is also important which has been established through rigorous calculations. In the context of atherosclerosis modeling, the diffusion term refers to the transport or movement of molecules such as lipids, immune cells, and inflammatory mediators within the arterial wall, while the reaction term represents the chemical involved in atherosclerosis, such as the oxidation of lipids, inflammation, and the formation of foam cells. These reactions are essential for plaque development and can influence the stability and vulnerability of plaques [24], [29]. To determine the conditions for measuring the inflammatory response over time we first analyze only the reaction part of a model (1)–(6).

3.1. The Reaction Dynamical System

The reaction dynamical ODE system is defined as,

$$\begin{aligned}
\frac{dM}{dt} &= \frac{\alpha_1 + \beta_1 P - \beta_2 A}{1 + \frac{(P+A)}{\tau_1}} - \lambda_1 M, \\
\frac{dP}{dt} &= \frac{\alpha_2 PM}{1 + \frac{A}{\tau_2}} + \delta\alpha_3 AM - \lambda_2 P, \\
\frac{dA}{dt} &= (1-\delta)\alpha_3 AM - \lambda_3 A.
\end{aligned} \tag{7}$$

In the next subsections, we have discussed the existence and uniqueness of the solution [30], [31], and after that, we calculated all possible equilibrium points of the reaction model (7).

3.2. Existence and Uniqueness of the Solution

In this subsection, we discussed the existence of solutions to this system of equations by the analytical method [30], [31], i.e., the Lipchitz condition [32], which showed that the solution is unique under derived conditions. Now, first, we simplified the equations of (7), and we get

$$M(t)-M(0)=\int_0^t\left[\frac{\alpha_1+\beta_1P(s)-\beta_2A(s)}{1+\frac{(P(s)+A(s))}{\tau_1}}-\lambda_1M(s)\right]ds=\int_0^t k_1\left(s,M,P,A\right)ds, \tag{8}$$

$$P(t)-P(0)=\int_0^t\left[\frac{\alpha_2P(s)M(s)}{1+\frac{A(s)}{\tau_2}}+\delta\alpha_3A(s)M(s)-\lambda_2P(s)\right]ds=\int_0^t k_2\left(s,M,P,A\right)ds, \tag{9}$$

$$A(t)-A(0)=\int_0^t\left[\left(1-\delta\right)\alpha_3A(s)M(s)-\lambda_3A(s)\right]ds=\int_0^t k_3\left(s,M,P,A\right)ds. \tag{10}$$

We consider the kernels, $k_1\left(t,M,P,A\right)=\dfrac{\alpha_1+\beta_1P-\beta_2A}{1+\frac{(P+A)}{\tau_1}}-\lambda_1M$, $k_2\left(t,M,P,A\right)=\dfrac{\alpha_2PM}{1+\frac{A}{\tau_2}}+\delta\alpha_3AM-\lambda_2P$ and $k_3\left(t,M,P,A\right)=\left(1-\delta\right)\alpha_3AM-\lambda_3A$ for simplification. Next, we shall prove that k_1, k_2 and k_3 satisfy Lipchitz's condition. Also, Consider $\|M\|=m=sup\{M,\forall t\in\Re^+\}$ and $\|A\|=a=inf\{A,\forall t\in\Re^+\}$. Therefore, for the first kernel $k_1\left(t,M,P,A\right)$, if $\lambda_1\leq\eta_1$,

$$\|k_1\left(t,M,P,A\right)-k_1\left(t,M_1,P,A\right)\|=|\lambda_1|\|M_1(t)-M(t)\|\leq\eta_1\|M(t)-M_1(t)\| \tag{11}$$

Similarly, we have taken the second and third kernels, and we get

$$\begin{aligned}\|k_2\left(t,M,P,A\right)-k_2\left(t,M,P_1,A\right)\|&=\|\left(\frac{\alpha_2PM}{1+\frac{A}{\tau_2}}+\delta\alpha_3AM-\lambda_2P\right)-\left(\frac{\alpha_2P_1M}{1+\frac{A}{\tau_2}}+\delta\alpha_3AM-\lambda_2P_1\right)\|\\&=\|\frac{\alpha_2M}{1+\frac{A}{\tau_2}}-\lambda_2\|\|P(t)-P_1(t)\|\\&\leq\eta_2\|P(t)-P_1(t)\|,\qquad if\quad\|\frac{\alpha_2m}{1+a/\tau_2}-\lambda_2\|\leq\eta_2.\end{aligned} \tag{12}$$

Finally, we check Lipchitz's condition for the third kernel k_3. So,

$$\begin{aligned}\|k_3\left(t,M,P,A\right)-k_3\left(t,M,P,A_1\right)\|&=\|\left(1-\delta\right)\alpha_3AM-\lambda_3A-\left(1-\delta\right)\alpha_3A_1M-\lambda_3A_1\|\\&=\|\left(1-\delta\right)\alpha_3M-\lambda_3\|\|A(t)-A_1(t)\|\\&\leq\eta_3\|A(t)-A_1(t)\|,\qquad if\quad\|\left(1-\delta\right)\alpha_3m-\lambda_3\|\leq\eta_3.\end{aligned} \tag{13}$$

Thus, we say that all the kernel functions satisfy Lipchitz's condition for some finite value of η_1,η_2 and η_3.

Theorem 3.1. *The reaction dynamical system (7) has a unique solution, iff* $\lambda_1\leq\eta_1$, $\|\dfrac{\alpha_2m}{1+a/\tau_2}-\lambda_2\|\leq\eta_2$, *and* $\|\left(1-\delta\right)\alpha_3m-\lambda_3\|\leq\eta_3$ *where* η_1,η_2 *and* η_3 *are some positive real numbers.*

Biological Interpretation: This Theorem 3.1 clearly shows that for the above conditions, the solution of the reaction-dynamical model has either non-inflammatory or inflammatory form of the disease. Two different possibilities never occurred at the same time.

3.3. Equilibrium Points

In this section, we calculated the equilibrium points for the steady state reaction dynamical system (7), and we get the following feasible equilibrium points [30], [33].

1) Non-inflammatory Equilibrium Point: After doing the calculation, we can see that non-inflammatory equilibrium point or cytokines free equilibrium point $E_0(\alpha_1/\lambda_1, 0, 0)$ exists without any condition, where the patient will recover from atherosclerosis without any influence of external biological affair. This shows that the patient survives without the disease if he or she follows a good routine and healthy diet.

2) Chronic Equilibrium Point: We also find another equilibrium point $E_1(M_1, P_1, A_1)$, where $M_1 = \lambda_2/\alpha_2, P_1 = K_1\tau_1/K_2, A_1 = 0$ with $K_1 = (\alpha_1\alpha_2 - \lambda_1\lambda_2)$, $K_2 = (\lambda_1\lambda_2 - \alpha_2\beta_1\tau_1)$, which exists where anti-inflammatory cytokines are not present in the arterial intima. This is called the chronic equilibrium point because atherosclerosis persists within the intima. The point will exist if either $K_1 > 0, K_2 > 0$ or $K_1 < 0, K_2 < 0$, where all parameters are positive.

3) Coexistence Equilibrium Point: The coexistence equilibrium point $E^*(M^*, P^*, A^*)$ is an extremely sensitive equilibrium point in which immune cells, pro-inflammatory cytokines, and anti-inflammatory cytokines persist. Such a case occurs when atherosclerosis increases or decreases over time in relation to the existing parameters. The existence and stability analysis of this equilibrium point is further discussed with the help of Bellman and Cooke's theorem [34], [35]. All these equilibrium states are biologically valid. The stability of these equilibrium points is discussed in the next section.

4. Stability Analysis of Equilibrium Points

As we know the stability of the equilibrium points is important for any dynamical model. After obtaining the non-inflammatory, chronic, and coexistence points we will now examine the stability of the equilibrium states. In the next subsections, we discuss the local stability analysis at these equilibrium points with the help of Lyapunov's first method and the global stability analysis with the help of Bellman and Cook's theorem.

4.1. Stability Analysis of Non-inflammatory Equilibrium Point

Lyapunov's first method is used to determine the local stability at the non-inflammatory equilibrium point (E_0). Initially, we define a Jacobian matrix for the system (7),

$$J(M,P,A) = \begin{pmatrix} -\lambda_1 & \frac{\beta_1}{1+\frac{A+P}{\tau_1}} - \frac{\alpha_1 - A\beta_2 + \beta_1 P}{\tau_1\left(1+\frac{A+P}{\tau_1}\right)^2} & -\frac{\beta_2}{1+\frac{A+P}{\tau_1}} - \frac{\alpha_1 - A\beta_2 + \beta_1 P}{\tau_1\left(1+\frac{A+P}{\tau_1}\right)^2} \\ \alpha_3\delta A + \frac{\alpha_2 P}{1+\frac{A}{\tau_2}} & \frac{\alpha_2 M}{1+\frac{A}{\tau_2}} - \lambda_2 & \alpha_3\delta M - \frac{\alpha_2 MP}{\tau_2\left(1+\frac{A}{\tau_2}\right)^2} \\ \alpha_3(1-\delta)A & 0 & \alpha_3(1-\delta)M - \lambda_3 \end{pmatrix}. \tag{14}$$

Now, the Jacobian at the point $E_0(\alpha_1/\lambda_1, 0, 0)$, becomes,

$$J(E_0) = \begin{pmatrix} -\lambda_1 & \beta_1 - \frac{\alpha_1}{\tau_1} & -\beta_2 - \frac{\alpha_1}{\tau_1} \\ 0 & \frac{\alpha_1\alpha_2}{\lambda_1} - \lambda_2 & \frac{\alpha_1\alpha_3\delta}{\lambda_1} \\ 0 & 0 & \frac{\alpha_1\alpha_3(1-\delta)}{\lambda_1} - \lambda_3 \end{pmatrix}. \tag{15}$$

After defining the characteristic equation for equation (15), we get

$$(\lambda + \lambda_1)\left(\lambda_1\left(\lambda + \lambda_2\right) - \alpha_1\alpha_2\right)\left(\lambda_1\left(\lambda + \lambda_3\right) - \alpha_1\alpha_3(1-\delta)\right) = 0, \tag{16}$$

where, λ is the eigenvalue of the Jacobian matrix (15) at E_0, which are $-\lambda_1, (\alpha_1\alpha_2 - \lambda_1\lambda_2)/\lambda_1$ and $(\alpha_1\alpha_3 - \delta\alpha_1\alpha_3 - \lambda_1\lambda_3)/\lambda_1$. Hence, it is stable if $\alpha_1/\lambda_1 < \lambda_2/\alpha_2$ and $\alpha_1/\lambda_1 < \lambda_3/(\alpha_3(1-\delta)))$.

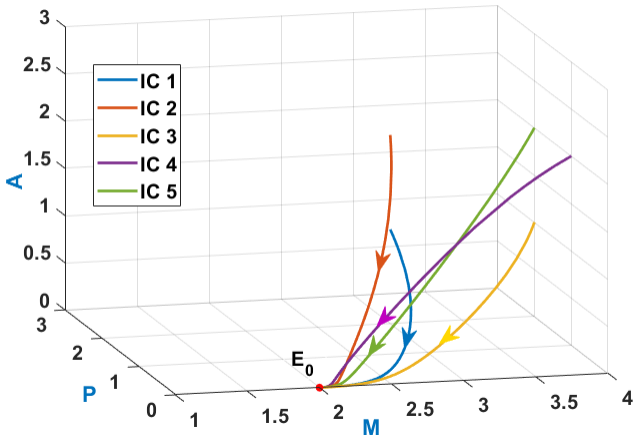

Figure 3: Stability of the non-inflammatory equilibrium pointE_0 when $\alpha_1/\lambda_1 < \min\{\lambda_2/\alpha_2, \lambda_3/(\alpha_3(1-\delta))\}$. The trajectories are obtained from the system (7) for different initial values of M, P and$A$.

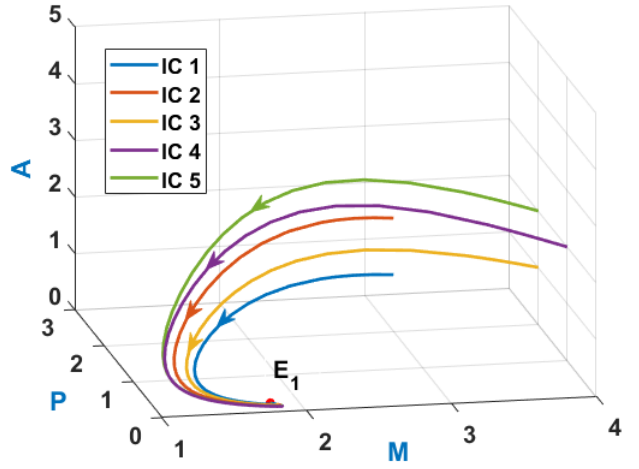

Figure 4: . Stability of the chronic equilibrium point E_1 when $\lambda_1/2 > \sqrt{K_1K_2/(K_1+K_2)}$ and $\lambda_2/\alpha_2 < \lambda_3/(\alpha_3(1-\delta))$. The trajectories are obtained from the system (7) for different initial values of M, P and A.

Theorem 4.1. *The reaction dynamical system (7) always has a non-inflammatory equilibrium point E_0, and it is stable if $\alpha_1/\lambda_1 < \min\{\lambda_2/\alpha_2, \lambda_3/(\alpha_3(1-\delta))\}$.*

Biological Interpretation: The above condition in theorem 4.1 confirms that if a low ox-LDL concentration is present in the intima region compared to cytokines level, there is no chance to trigger chronic inflammation. The inflammation will definitely disappear.

4.2. Stability Analysis of Chronic Equilibrium Point

Now, we define the characteristic equation from equation (14) at chronic equilibrium point,

$$(\alpha_2(\lambda+\lambda_3)-\alpha_3(1-\delta)\lambda_2)\left(K_1^2\lambda(\lambda+\lambda_1)+K_2^2\lambda(\lambda+\lambda_1)+K_1K_2(\alpha_1\alpha_2+2\lambda(\lambda+\lambda_1)-\alpha_2\beta_1\tau_1)\right)=0, \tag{17}$$

where, λ is the root of the equation (17), which are $-\frac{\lambda_1}{2}\pm\sqrt{\left(\frac{\lambda_1}{2}\right)^2-\frac{K_1K_2}{(K_1+K_2)}}$ and $\frac{\alpha_2\lambda_3-\alpha_3(1-\delta)\lambda_2}{\alpha_2}$.

Case – I: If $K_1>0, K_2>0$

A) When $\frac{\lambda_1}{2}<\sqrt{\frac{K_1K_2}{(K_1+K_2)}}$ and $\frac{\lambda_2}{\alpha_2}<\frac{\lambda_3}{\alpha_3(1-\delta)}$, then one pair of eigenvalues of the equation (17) must be complex with negative real parts. Hence, the equilibrium point will be asymptotically stable.

B) When $\frac{\lambda_1}{2}>\sqrt{\frac{K_1K_2}{(K_1+K_2)}}$ and $\frac{\lambda_2}{\alpha_2}<\frac{\lambda_3}{\alpha_3(1-\delta)}$, then all the eigenvalues of the equation (17) must be negative. Hence, the equilibrium point will be stable.

Case – II: If $K_1<0, K_2<0$, then at least one eigenvalues of the equation (17) must be positive. Hence, the equilibrium point will be unstable.

4.3. Stability Analysis of Coexistence Equilibrium Point

It is very tedious to examine the stability of the coexistence equilibrium point $E^*(M^*,P^*,A^*)$ analytically. For this reason, we used Bellman and Cooke's theorem to determine global stability.

Bellman and Cooke's Theorem

Let $\Im(z)=\mu(z,e^z)$, where $\mu(z,e^z)$ is a polynomial with principal term. The function $\Im(iw)$ is now separated into real and imaginary parts, i.e., we set $\Im(iw)=\phi(w)+i\psi(w)$. If all the zeros of the function $\Im(z)$ lie to the left side of the imaginary axis, the zeros of the functions $\phi(w)$and $\psi(w)$are real, alternating and for each w,

$$\phi(w)\psi^{'}(w)-\phi^{'}(w)\psi(w)>0. \tag{18}$$

In addition, in order that all the zeros of the function lie to the left of the imaginary axis, it is sufficient that one of the following conditions be satisfied.

a) All the zeros of the functions $\phi(w)$and $\psi(w)$ are real and alternating and the inequality (18) satisfied for at least one value of w.

b) All the zeros of the function $\phi(w)$ are real and for each zeros $w=w_0$ condition (18) is satisfied. i.e. $\phi^{'}(w)\psi(w)<0$.

c) All the zeros of the function $\psi(w)$ are real and for each zeros $w=w_0$ inequality (18) satisfied. i.e. $\phi(w)\psi^{'}(w)>0$.

After making the necessary calculations to find out the characteristic equation of the Jacobian matrix (14) at $E^*(P^*,A^*,M^*)$, we define $\Im(z)$. Next, we determine the Bellman coefficient, $B(w)=\phi(w)\psi^{'}(w)-\phi^{'}(w)\psi(w)$ for every real value of w. Now, setting $w=0$, we have $\phi^{'}(0)=0$ and $\psi(0)=0$. Hence, $B(0)=\phi(0)\psi^{'}(0)$. Now, for the equilibrium point $E^*(M^*,P^*,A^*)$, B becomes,

$$\begin{aligned}B(E^*)=&\frac{[129(69+\theta)+\delta(-31557-218\theta+\delta(31980+\delta-(18343-7519\delta)+109\theta))]}{[332750(69-49\delta)^2(-1+\delta)^5]}[-2070(69+\theta)\\&+\delta(613341+11811\theta-\delta(312315+23188\theta-\delta\{\delta(3774755-\delta(3194025-1087849\delta)-7301\theta)\\&-27(71825-824\theta)))\}]\end{aligned}$$

where $\theta=\sqrt{((4761+\delta(-26634+\delta(52811-\delta(47514-22201\delta)))))}$.

And according to the third condition of Bellman and Cooke, the equilibrium point E^* will be stable when B is greater than zero. Now for different values of δ, we find that the Bellman coefficient, B, shows interesting results, which are presented in Table 2. This Table 2 clearly demonstrates that the Bellman coefficient is decreasing with increase of δ and it changes the sign after the value of $\delta=0.5$. Hence, this observation shows that the point $E^*(M^*,P^*,A^*)$ will be stable before $\delta<0.5$, otherwise, it is unstable.

Table 2: Behaviour of Bellman coefficient at coexisting equilibrium point $E^*(M^*, P^*, A^*)$ for various values of δ, and different parameter values taken from Table 3.

δ	B	*Stability*
0.31	0.29991	Stable
0.35	0.13254	Stable
0.39	0.03654	Stable
0.43	0.00274	Stable
0.47	0.00008	Stable
0.51	-0.00272	Unstable
0.55	-0.06476	Unstable
0.59	-0.37836	Unstable

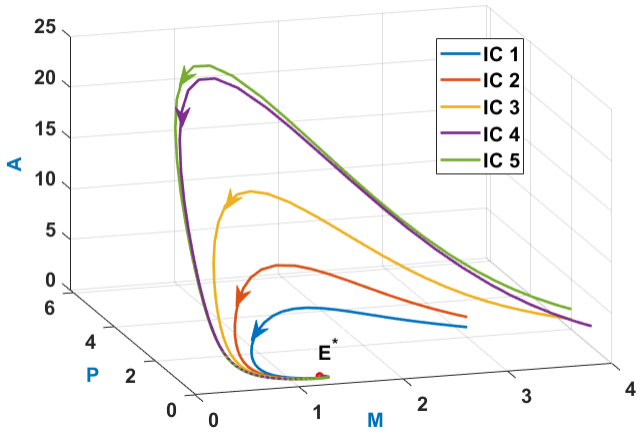

Figure 5: Stability of co-existence equilibrium point E^* for different parameter values, taken from Table 3. The trajectories are obtained from the system (7) for different initial values of M, P, and A.

5. Numerical Simulation and Discussion

In this section, we have demonstrated the effectiveness of the proposed theoretical results with validation studies from the numerical solution of the atherosclerosis model. The numerical simulations of the model (1)-(6) are carried out with the help of MATHEMATICA software through NDSolve using Runge-Kutta fourth-order method. In various studies [29], [36], [37], we found that the initial conditions are defined as a smooth function of x due to experimentally observed results. Here also we choose the smooth functions of x for the initial conditions, $M_0(x) = 2 + 2e^{-(0.1x-5)^2}$, $P_0(x) = 2e^{-(0.1x-5)^2}$ and $A_0(x) = 2e^{-(0.1x-5)^2}$.

5.1. Numerical Simulation for Non-Inflammatory Equilibrium Point

In this subsection, we discuss the numerical simulation of the model (1)-(6) for the first set of data taken from Table 3. This data has been considered for low concentrations of ox-LDL and cytokines in the intima. Figure 6 clearly shows that initial perturbation in immune cells and cytokines has not impacted. Therefore, the concentration of immune cells, pro, and anti-cytokines rapidly approaches to non-inflammatory equilibrium point $E_0(2, 0, 0)$, with the increase of time, which means that the inflammation disappears in a very short time. Hence, we say that the inflammation will vanish if we ensure the inequality $\frac{\alpha_1}{\lambda_1} < \min\{\frac{\lambda_2}{\alpha_2}, \frac{\lambda_3}{\alpha_3(1-\delta)}\}$ is satisfied.

Table 3: Parameter values for stability at different equilibrium points.

Parameters	E_0	E_1	E^*	References
α_1	2	2	2	[29], [36], [37]
α_2	1	1	1	[29], [36], [37]
α_3	1	1	2	[38]
β_1	5	1	1	[29]
β_2	1	0.2	0.2	Estimated
λ_1	1	1	1	[29], [37]
λ_2	4	1.8	1.8	Estimated
λ_3	4	2	2	Estimated
τ_1	1	1	1	[29], [37]
τ_2	$\frac{42}{43}$	$\frac{42}{43}$	1	[36], [38]
δ	0.2	0.2	0.2	Estimated
d_1	1	1	1	[29]
d_2	1	1	1	[29]
d_3	1	1	1	[29]
$M_0(x)$	$2+2e^{-(0.1x-5)^2}$	$2+2e^{-(0.1x-5)^2}$	$2+2e^{-(0.1x-5)^2}$	[37]
$P_0(x)$	$2e^{-(0.1x-5)^2}$	$2e^{-(0.1x-5)^2}$	$2e^{-(0.1x-5)^2}$	[37]
$A_0(x)$	$2e^{-(0.1x-5)^2}$	$2e^{-(0.1x-5)^2}$	$2e^{-(0.1x-5)^2}$	[37]

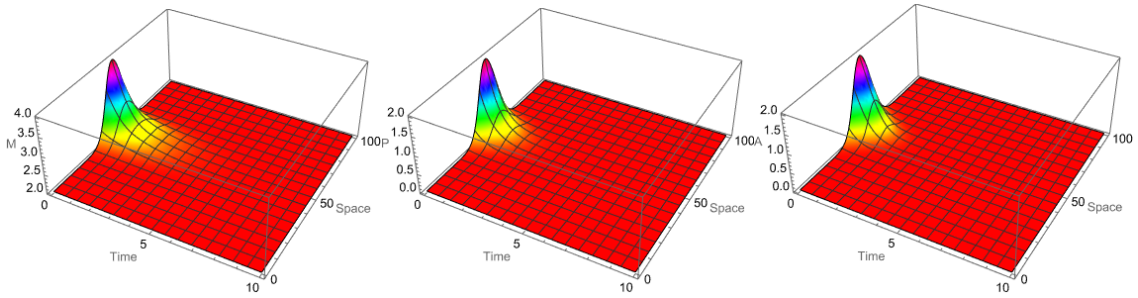

(i) (ii) (iii)

Figure 6: Behaviour of concentration of i) immune cells (M), ii) pro-inflammatory cytokines (P) and iii) anti-inflammatory cytokines with respect to space variable (x) and time (t) for parameter's values taken from Table 3.

.

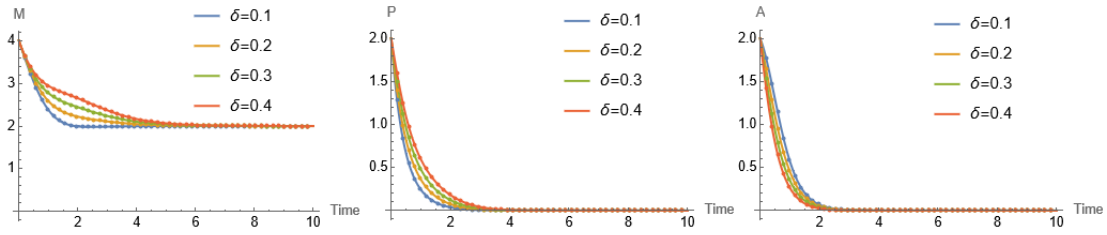

(i) (ii) (iii)

Figure 7: Plot of concentration functions vs. time for different values of $\delta = 0.1, 0.2, 0.3, 0.4$ at $x = 50$ and other parameter's values taken from Table 3.

.

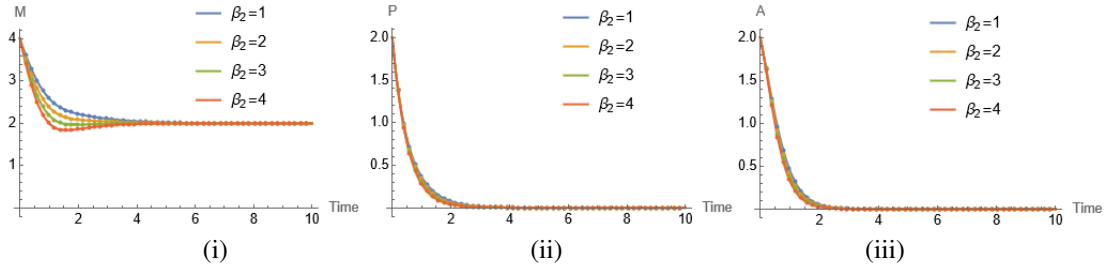

Figure 8: Plot of concentration functions vs. time for different values of $\beta_2 = 1, 2, 3, 4$ at $x = 50$ and other parameter's values taken from Table 3.

.

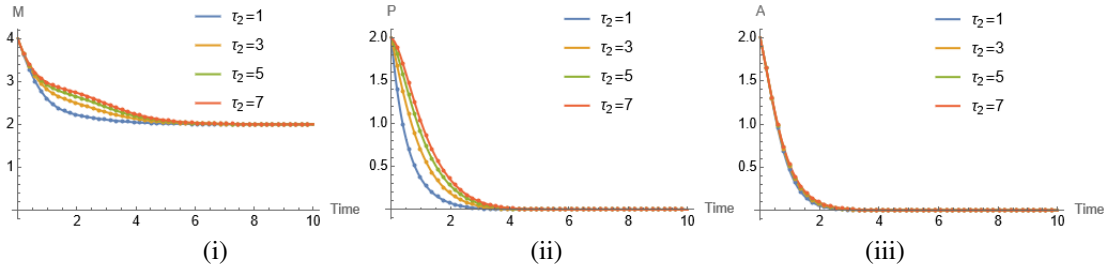

Figure 9: Plot of concentration functions vs. time for different values of $\tau_2 = 1, 3, 5, 7$ at $x = 50$ and other parameter's values taken from Table 3.

.

Figure 7(i) depicts that the concentration of immune cells decreases over time and tends to α_1/λ_1, in addition, it increases with the increase of δ. Similarly, Figure 7(ii) shows that the concentration of pro-cytokines decreases over time and tends to 0, and it increases with the increase of δ. However, Figure 7(iii) demonstrates that the concentration of anti-cytokines decreases over time and tends to 0, although it decreases with the increase of δ. In Figure 8(i), it is described that initially the concentration of immune cells decreases exponentially and crosses the level of equilibrium point but as time passes it recovers slowly and reaches the equilibrium point α_1/λ_1. It is also observed that immune cells decrease with the increase of β_2. Similarly, Figures 8(ii) and 8(iii) illustrate that the concentration of both cytokines decreases over time and tends to 0, and they increase slowly with the increase of β_2. Figure 9 shows the variation of M and P in a similar fashion as it was plotted for δ. Figure 9(i), the concentration of immune cells has been shown to decrease over time and it tends to α_1/λ_1, it also assures that the concentration of the same increases with the increase of τ_2. Figure 9(ii) shows that the concentration of pro-cytokines decreases over time and tends to 0, and it increases with the increase of τ_2. On the other hand, Figure 9(iii) demonstrates that the concentration of anti-cytokines decreases over time and it tends to 0. However, it exhibits almost no variation with the increase of τ_2.

5.2. Numerical Simulation for Chronic Equilibrium Point

In this subsection, we discuss the numerical simulation of the model (1)-(6) for the second set of data taken from Table 3. This data stands for high concentration of ox-LDL and moderate concentration of cytokines in the intima, and the above analytical study suggests that this chronic inflammatory point, $E_1(M_1, P_1, A_1)$, is stable. Figure 10 evidently demonstrates the behaviour of concentrations with respect to length (x) and time (t). Figure 10(i) shows that initially the immune cells decrease very quickly and drop below the equilibrium level but after some time it recovers and reach the equilibrium point. Figure 10(ii) demonstrates that in a very short time, the concentration of pro-cytokines increases thereafter it decreases over time and tends to equilibrium

point. Figure 10(iii) represents that for the initial time the concentration of pro-cytokines increases thereafter it decreases over time and tends to equilibrium point. So, the numerical simulation assures that the system exhibits a threshold effect to reach its equilibrium point over time. We can see that no anti-inflammatory cytokines exist to suppress the propagation of inflammation. Hence, we say that the inflammation will trigger chronic disease if the inequalities $\lambda_1/2 > \sqrt{K_1K_2/(K_1+K_2)}$ and $\lambda_2/\alpha_2 < \lambda_3/(\alpha_3(1-\delta))$ are satisfied.

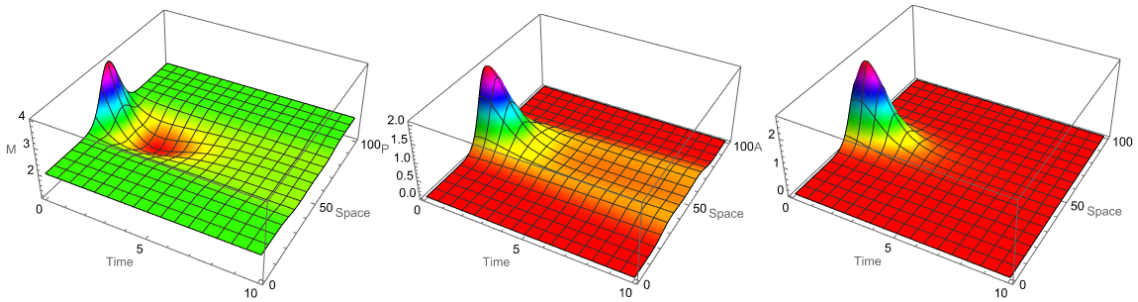

(i) (ii) (iii)

Figure 10: Behavior of concentration of i) Immune cells (M), ii) Pro-inflammatory cytokines (P) and iii) Anti-inflammatory cytokines with respect to space variable (x) and time (t) for values of parameter taken from Table 3.

.

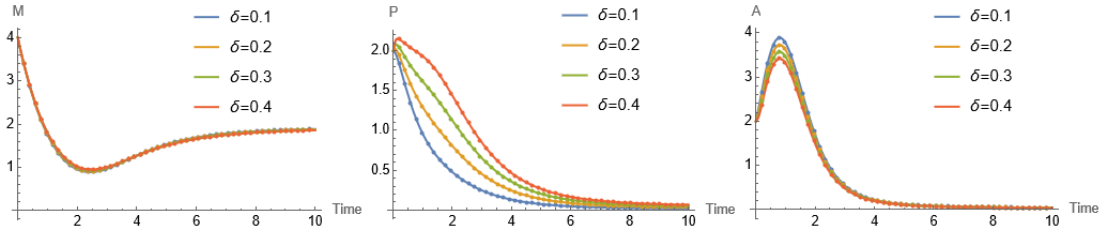

(i) (ii) (iii)

Figure 11: Plot of concentration functions vs. time for different values of $\delta = 0.1, 0.2, 0.3, 0.4$ at $x = 50$ and other parameter's values taken from Table 3.

.

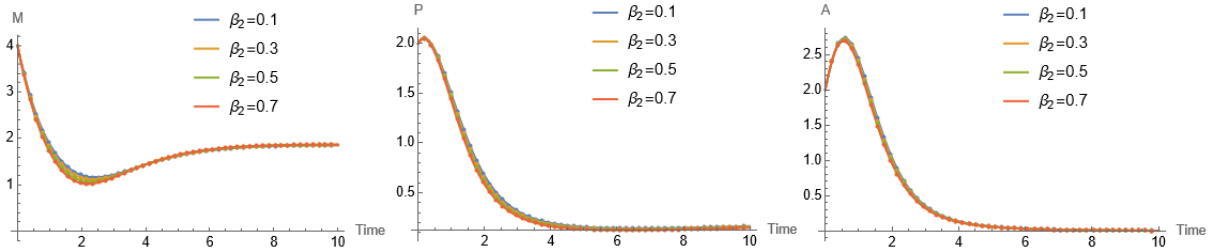

(i) (ii) (iii)

Figure 12: Plot of concentration functions vs. time for different values of $\beta_2 = 0.1, 0.3, 0.5, 0.7$ at $x = 50$ and other parameter's values taken from Table 3.

.

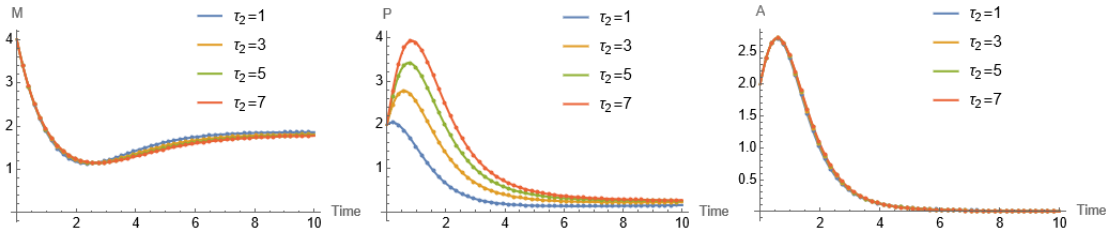

Figure 13: Plot of concentration functions vs. time for different values of $\tau_2 = 1, 3, 5, 7$ at $x = 50$ and other parameter's values taken from Table 3.

.

Figure 11(i) shows that the concentration of immune cells decreases over time and goes down to a certain depth and then it increases and it tends to M_1, but it exhibits almost no variation with the increase of δ. In Figure 11(ii), the concentration of pro-cytokines gives a little hike and very soon it decreases over time and eventually approaches to P_1, however, it increases with the increase of δ. Also, Figure 11(iii) demonstrates that the concentration of anti-cytokines first increases very fast for a certain time then it decreases and tends to A_1, although it decreases with the increase of δ. Figure 12(i) displays that the concentration of immune cells decreases very quickly and drops below the equilibrium level then again after some time it rises and reaches to M_1. Yet, the concentration increases with the increase of β_2. In Figure 12(ii), the pro-cytokines initially increase a little bit and very soon decrease and eventually approach to over time, also it decays in very small quantity with the increase of β_2. On the other hand, Figure 12(iii) reveals that the concentration of anti-inflammatory cytokines primarily increases for a certain time, then it decreases and tends to A_1. However, it exhibits almost no variation with the increase of β_2. In Figure 13(i), it is described that initially the concentration of immune cells decreases and crosses the level of equilibrium point but as time spends it upturns and reaches the equilibrium point M_1. It is also detected that immune cells decrease with the increase of τ_2. Unlike, Figure 13(ii) shows that the concentration of pro-cytokines initially upturns and tends to P_1 over time and it increases with the increase of τ_2. On the other hand, Figure 13(iii) does not show any variation in the concentration of anti-inflammatory cytokines with the increase of τ_2. But the curve initially rises then steadily decays over time and tends to A_1.

5.3. Numerical Simulation of Coexistence Equilibrium Point

In this subsection, the numerical simulation of the presented inflammatory model is displayed for the third set of data of Table 3. This data set corresponds to the medical condition with a high concentration of ox-LDL, medium concentration of pro-inflammatory cytokines, and high concentration of anti-cytokines in the intima. The analytical study assures that this coexistence equilibrium point $E^*(M^*, P^*, A^*)$ is stable if $\delta < 0.5$. This coexistence state E^* is the most concerned equilibrium point in this study. The behaviour of concentration with respect to length (x) and time (t) is shown clearly in Figure 14. Figure 14(i) describes that initially the concentration of immune cells decreases very quickly and drops below the equilibrium level but after some time it recovers and reaches the equilibrium point M^*. Figure 14(ii) demonstrates that in a very short time, the concentration of pro-cytokines increases thereafter it decreases over time and tends to equilibrium point P^*. Figure 14(iii) represents that initially the concentration of pro-cytokines increases thereafter it decreases over time and tends to equilibrium point A^*. If we choose $\delta > 0.5$, for the same set of data the scenario will be different. In Figure 15, it is shown that the concentrations do not tend to $E^*(M^*, P^*, A^*)$, rather it approaches to choric equilibrium point $E_1(M_1, P_1, A_1)$. Figure 14(i) expresses that the concentration of immune cells decreases over time and goes down to a certain level and then it increases. Eventually, it tends to M^*, while $\delta > 0.5$ and approaches to M_1 for $\delta > 0.5$.

Moreover, the concentration increases with the increase of δ. In Figure 15(ii), the concentration of pro-cytokines at first increases exponentially, and then after an interval of time it decreases in a very opposite manner and ultimately approaches P^*, while $\delta < 0.5$ and approaches P_1 for $\delta > 0.5$. However, the same

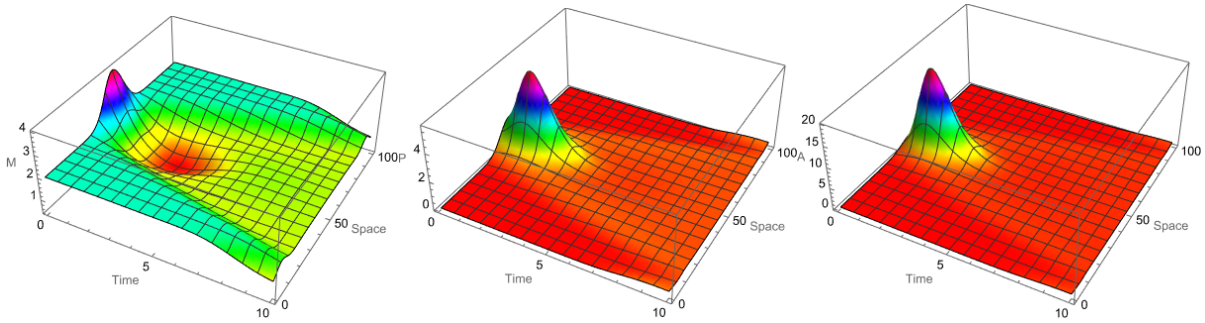

(i) (ii) (iii)

Figure 14: Behavior of concentration of i) Immune cells (M), ii) Pro-inflammatory cytokines (P), and iii) Anti-inflammatory cytokines with respect to space variable (x) and time (t) for values of parameter taken from Table 3.

.

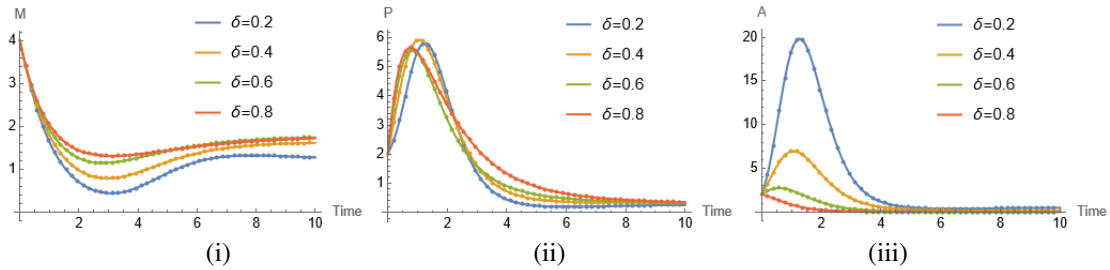

(i) (ii) (iii)

Figure 15: Plot of concentration functions vs. time for different values of $\delta = 0.2, 0.4, 0.6, 0.8$ at $x = 50$ and other parameter's values taken from Table 3.

.

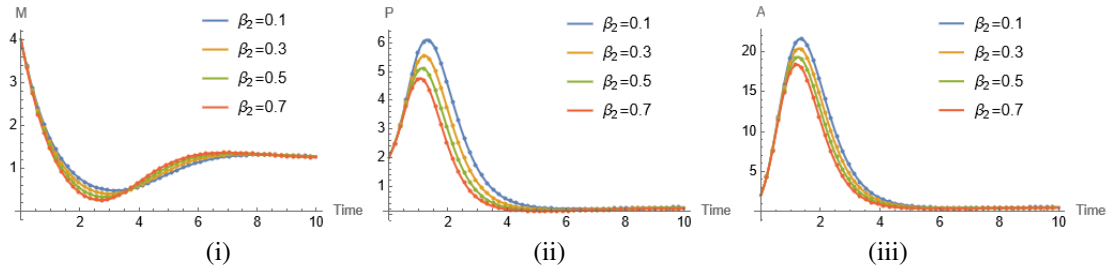

(i) (ii) (iii)

Figure 16: Plot of concentration functions vs. time for different values of $\beta_2 = 0.1, 0.3, 0.5, 0.7$ at $x = 50$ and other parameter's values taken from Table 3.

.

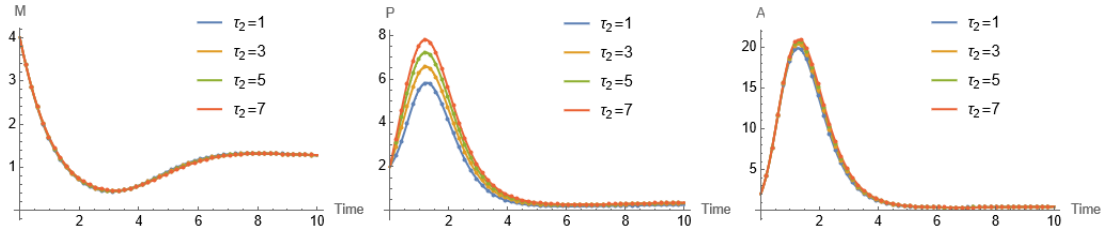

Figure 17: Plot of concentration functions vs. time for different values of $\tau_2 = 1, 3, 5, 7$ at $x = 50$ and other parameter's values taken from Table 3.

.

increases with the increase of δ. Also, Figure 15(iii) demonstrates that the concentration of anti-cytokines first rises extremely fast up to a high point over time then it decreases and tends to A^*, while $\delta < 0.5$ and converges to A_1 for $\delta > 0.5$. Even though it decreases with the increase of δ. Figure 16(i) displays that the concentration of immune cells decreases very quickly and drops below equilibrium point then after some time it rises. Yet, the concentration decreases initially and then increases with the increase of β_2. In Figures 16(ii) and 16(iii) the pro- and anti-inflammatory cytokines initially increase up to a high level and after an interval of time, they both decrease and eventually approach its equilibrium point. Also, they decrease in a very similar fashion with the increase of β_2. In Figures 17(i) and 17(iii), immune cells and anti-inflammatory cytokines almost show no variation as τ_2 increases. But they tend to M^* and A^* respectively over time. On the other hand, pro-inflammatory cytokines in Figure 17(ii), grow at a certain level but as time spends decreases and reach P^*. It is also noticed that the concentration of immune cells increases with the increase of τ_2. Due to the presence of high- high-concentration ox-LDL and high- high-concentration anti-inflammatory cytokines the system has to overcome a threshold effect. This case is very much sensitive to its parameters, especially δ. Some change of δ, can make the scenario different. Figure 14 and Figure 18, illustrate this very important fact showing the behavior of concentrations with respect to x and t. We can see for $\delta = 0.2$, immune cells, pro-inflammatory cytokines, and anti-inflammatory cytokines tend to $1.25, 0.2491$, and 0.4743, respectively.

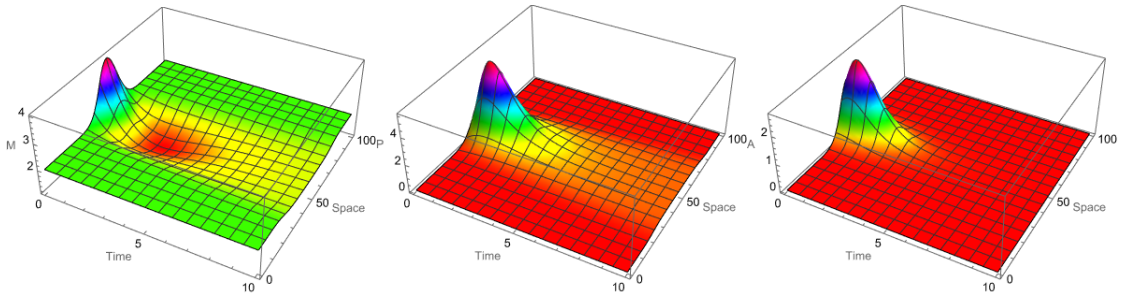

Figure 18: Behavior of concentration of i) Immune cells (M), ii) Pro-inflammatory cytokines (P), and iii) Anti-inflammatory cytokines with respect to space variable (x) and time (t) for $\delta = 0.6$ values of parameters taken from Table 3.

.

However for $\delta = 0.6$, immune cells, pro-inflammatory cytokines, and anti-inflammatory cytokines tend to $1.8, 0.25, 0$, respectively. Hence, we say that $E^*(1.25, 0.2491, 0.4743)$ will be unable to hold the stability and shift to the chronic inflammatory point $E_1(1.8, 0.25, 0)$. This transformation of the equilibrium point is shown in a more specific way in Figure 15.

6. Conclusions

In this article, a reaction-diffusion atherosclerosis model is developed with three different compartments viz. immune cells, pro-inflammatory cytokines, and anti-inflammatory cytokines. This study provides insight into the effects of pro- and anti-inflammatory cytokines in atherosclerosis with the help of a deterministic model. Anti-inflammatory cytokines play an important role in controlling atherosclerosis propagation. But in various studies [27], [28], sometimes few anti-cytokines (TGF-beta, IL-6) have shown opposite characteristics, and behave like pro-inflammatory cytokines. In the proposed model, we consider some anti-cytokines to behave like pro-cytokines, therefore assumed to be there, and denoted with δ. This behavior shows a significant novel impact in this study and provides new insights for the visualization of atherosclerosis. The proposed mathematical model is investigated analytically and numerically. The analytical study suggests that the solutions are unique and stable at non-inflammatory, chronic, and coexistence equilibrium states for a particular set of parameters. Global stability is illustrated through Bellman and Cooke's stability method at the coexistence equilibrium point. We validated and compared analytical results with numerical results [29], [37], which is depicted through Figures 3-18. This study provides three main results; the first one is, that if the intima contains a low concentration of ox-LDL, the dissemination of chronic inflammation does not result from disturbances in the non-inflammatory state, i.e., no chronic inflammation will trigger and the body will recover soon. The second consequence is that when a high concentration of ox-LDL and a moderate concentration of pro and anti-cytokines are present in the intima, inflammation will increase and reach the stage of chronic atherosclerosis. Another possibility is that if a high concentration of ox-LDL, moderate concentration of pro-cytokines, and high concentration of anti-cytokines are available in the intima, inflammation will increase and approach a coexistence equilibrium state and a very less possibility of reaching the stage of chronic atherosclerosis. Hence, a patient will stay alive with the disease in the midst of an uneasy lifestyle. Thus, the results clearly indicate that the patient can avoid the chronic condition if the patient takes a regular and healthy diet with proper medication.

Acknowledgement

The authors are highly thankful to the unknown referees for their valuable comments and suggestions.

References

[1] WHO, Fact Sheet, Details of Cardiovascular-Diseases, 11 June 2021, https://www.who.int/news-room/fact-sheets/detail/cardiovascular-diseases-(cvds).

[2] Diaz, A., Bourassa, M.G., Guertin, M.C. and Tardif, J.C., Long-term prognostic value of resting heart rate in patients with suspected or proven coronary artery disease, Eur. Heart J, 26(10), pp. 967-974, 2005.

[3] Rodriguez, A.D., Palacios, G.B. and Gonzalez, P.A., Increased heart rate and atherosclerosis: Potential implications of ivabradine therapy, World J. Cardiol., 3(4), pp. 101–104, 2011.

[4] Li, X, Gu, J, Xiao, Q, Liu, Y., Zhou, P., Fan, L., Zhang, X., Lu, X., Wu, J., Liu, Z. and He, W., Liposomal codelivery of inflammation inhibitor and collagen protector to the plaque for effective anti-atherosclerosis, Chinese Chemical Letters, 34(1), pp. 107483, 2023.

[5] Sacks, F.M., Lichtenstein, A.H., Wu, J.H.Y., Appel, L.J., Creager, M.A. and Kris-Etherton, P.M., Dietary fats and cardiovascular disease: a presidential advisory from the American Heart Association, Circulation, 136(3), pp. e1–23, 2017.

[6] Lian, Z., Perrard, X. Y. D., Peng, X., Raya, J. L., Hernandez, A. A., Johnson, C. G., Wu, H. Replacing saturated fat with unsaturated fat in Western diet reduces foamy monocytes and atherosclerosis in male Ldlr–/–mice, Arteriosclerosis, thrombosis, and vascular biology, 40(1), pp. 72-85, 2020.

[7] Ilias, N., Hamzah, H., Ismail, I. S., Mohidin, T. B. M., Idris, M. F., and Ajat, M, An insight on the future therapeutic application potential of Stevia rebaudiana Bertoni for atherosclerosis and cardiovascular diseases. Biomedicine & Pharmacotherapy, 143, pp. 112207, 2021.

[8] Moghaddam, P.M., Ghobadian, R. and Ahangar, H.K., Dementia in diabetes mellitus and atherosclerosis: Two interrelated systemic diseases, Brain Res. Bull., 181, pp. 87-96, 2022.

[9] Koskinas, K.C., What is the role of lipids in atherosclerosis and how low should we decrease lipid levels? e-Journal of Cardiology Practice, 19(1), pp. 1-15, 2020.

[10] Maiolino, G., Rossitto, G., Caielli, P., Bisogni, V., Rossi, G. P. and Calò, L.A., The role of oxidized low-density lipoproteins in Atherosclerosis: The Myths and the Facts, Mediators Inflamm., (2013), pp. 714653, 2013.

[11] Steinbrecher, U.P., Parthasarathy, S. and Leake, D.S., Modification of low density lipoprotein by endothelial cells involves lipid per oxidation and degradation of low density lipoprotein phospholipids, Proceedings of the National Academy of Sciences, United States of America, 81(12), pp. 3883-3887, Jun. 1984.

[12] Henriksen, T., Mahoney, E.M. and Steinberg, D., Enhanced macrophage degradation of biologically modified low density lipoprotein, Arteriosclerosis: An Official Journal of the American Heart Association, Inc., 3(2), pp.149-159, 1983.

[13] Heinecke, J.W., Rosen, H. and Chait, A., Iron and copper promote modification of low density lipoprotein by human arterial smooth muscle cells in culture, Journal of Clinical Investigation, 74(5), pp.1890–1994, 1984.

[14] Tousoulis, D., Oikonomou, E., Evangelos, K. E., Crea, F. and Kaski, J.C., Inflammatory cytokines in atherosclerosis: current therapeutic approaches, European Heart Journal, 37(22), pp.1723-1732, 2016.

[15] Oufella, H.A., Taleb, S., Mallat, Z. and Tedgui, A., Recent advances on the role of cytokines in Atherosclerosis, Arteriosclerosis, Thrombosis, and Vascular Biology, 31(5), pp. 969–979, 2011.

[16] Hafiane, A. and Daskalopoulou, S. S., Targeting the residual cardiovascular risk by specific anti-inflammatory interventions as a therapeutic strategy in atherosclerosis, Pharmacological Research, 178, p. 106157, 2022.

[17] Roesner, C., Goeller, M., Schrauder, D.R., Dey, D., Kilian, T., Achenbach, S., Marwan, Md. and Bittner, D.O., Differences of inflammatory cytokine profile in patients with vulnerable plaque: A coronary CTA study, Atherosclerosis, 350, pp. 25-32, 2022.

[18] Fatkhullina, A.R, Peshkova, I.O. and Koltsova, E.K., The role of cytokines in the development of Atherosclerosis, Biochemistry (Mosc), 81(11), pp. 1358–1370, 2016.

[19] Lutgens, E., Joffre, J., van Os, B. and Ait-Oufella, H., Targeting cytokines and immune checkpoints in atherosclerosis with monoclonal antibodies, Atherosclerosis, 335, pp. 98-109, 2021.

[20] Biros, E., Reznik, J.E. and Moran, C.S., Role of inflammatory cytokines in genesis and treatment of atherosclerosis, Trends in Cardiovascular Medicine, 32(3), pp. 138-142, 2022.

[21] Kirichenko, T.V., Sobenin, I.A., Nikolic, D., Rizzo, M. And Orekhov, A.N., Anti-cytokine therapy for prevention of atherosclerosis, Phytomedicine, 23(11), pp. 1198-1210, 2016.

[22] Cantrell, R.S. And Cosner, C., On the dynamics of predator–prey models with the Beddington–DeAngelis functional response, Journal of Mathematical Analysis and Applications, 257(1), pp. 206-222, 2001.

[23] Ji, J. and Wang, L., Competitive exclusion and coexistence in an intraguild predation model with Beddington–DeAngelis functional response, Communications in Nonlinear Science and Numerical Simulation, 107, p. 106192, 2022.

[24] Chalmers, A.D., Bursill, C.A. and Myerscough, M. R., Nonlinear dynamics of early atherosclerotic plaque formation may determine the efficacy of high-density lipoproteins (HDL) in plaque regression, PLoS One, 12(11), p. e0187674, 2017.

[25] Arango, D.G. and Descoteaux, A., Macrophage cytokines: involvement in immunity and infectious diseases, Frontiers in immunology, 5, pp, 491, 2014.

[26] Barrett, T.J., Macrophages in atherosclerosis regression, Arteriosclerosis, thrombosis, and vascular biology, 40(1), pp. 20-33, 2020.

[27] Chen, P.Y., Qin, L., Li, G., Wang, Z., Dahlman, J.E., Lopez, J.M., Gujja et al., Endothelial TGF$-\beta$ signalling drives vascular inflammation and atherosclerosis, Nature metabolism, 1(9), pp. 912-926, 2019.

[28] Scheller, J., Chalaris, A., Arras, D.S. and Rose-John, S., The pro-and anti-inflammatory properties of the cytokine interleukin-6, Biochimica et Biophysica Acta (BBA)-Molecular Cell Research, 1813(5), pp. 878-888, 2011.

[29] El Khatib, N., Génieys, S. and Volpert, V., Atherosclerosis initiation modeled as an inflammatory process, Mathematical Modelling of Natural Phenomena, 2(2), pp. 126-141, 2007.

[30] Deo, S.G. and Raghvendra, V., Ordinary differential equations and stability theory, Tata McGraw-Hill Publishing Company Limited, New Delhi, 1988.

[31] Singh, J., Kumar, D., Hammouch, Z. and Atangana, A, A fractional epidemiological model for computer viruses pertaining to a new fractional derivative, Applied Mathematics and Computation, 316, pp. 504-515, 2018.

[32] Gupta, P.K. and Adak, A., A study of the Caputo-Fabrizio fractional model for Atherosclerosis disease. In Proceedings of the International Conference on Computational Intelligence and Sustainable Technologies: ICoCIST 2021, Singapore: Springer Nature Singapore, pp. 19-29, 2022.

[33] Gupta, P.K. and Dutta, A., A mathematical model on HIV/AIDS with fusion effect: Analysis and homotopy solution, The European Physical Journal Plus, 134(6), p. 265, 2019.

[34] Bellman, R. and Cooke, K.C., Differential difference equation, Academic Press, London, UK, 1963.

[35] Dutta, A. and Gupta, P.K, Stability analysis of HIV/AIDS dynamics: Modelling the tested and untested populations, Pramana - J. Phys., 96(1), p. 42, 2022.

[36] EL Khatib, N., Genieys, S., Kazmierczak, B. and Volpert, V., Reaction diffusion model of atherosclerosis development, Journal of Mathematical Biology, 65(2), pp. 349-374, 2012.

[37] Hidalgo, A., Tello, L. and Toro, E.F., Numerical and analytical study of an atherosclerosis inflammatory disease model, Journal of Mathematical Biology, 68(7), pp. 1785-1814, 2014.

[38] Chow, C.C., Clermont, G., Kumar, R., Lagoa, C., Tawadrous, Z., Gallo, D., Betten, B., Bartels, J., Constantine, G., Fink, M.P. and Billiar, T.R., The acute inflammatory response in diverse shock states, Shock, 24(1), pp. 74-84, 2005.